

Ferroelectrics

Ferroelectric and Spin Crossover Behavior in a Cobalt(II) Compound Induced by Polar-Ligand-Substituent Motion

Ryohei Akiyoshi, Yuki Komatsumaru, Masaki Donoshita, Shun Dekura, Yukihiko Yoshida, Hiroshi Kitagawa, Yasutaka Kitagawa, Leonard F. Lindoy, and Shinya Hayami*

Abstract: Ferroelectric spin crossover (SCO) behavior is demonstrated to occur in the cobalt(II) complex, $[\text{Co}(\text{FPh-terpy})_2](\text{BPh}_4)_2 \cdot 3\text{ac}$ (**1-3 ac**; FPh-terpy = 4'-((3-fluorophenyl)ethynyl)-2,2':6,2''-terpyridine) and is dependent on the degree of 180° flip–flop motion of the ligand's polar fluorophenyl ring. Single crystal X-ray structures at several temperatures confirmed the flip–flop motion of fluorobenzene ring and also gave evidence for the SCO behavior with the latter behavior also confirmed by magnetic susceptibility measurements. The molecular motion of the fluorobenzene ring was also revealed using solid-state ^{19}F NMR spectroscopy. Thus the SCO behavior is accompanied by the flip–flop motion of the fluorobenzene ring, leading to destabilization of the low spin cobalt(II) state; with the magnitude of rotation able to be controlled by an electric field. This first example of spin-state conversion being dependent on the molecular motion of a ligand-appended fluorobenzene ring in a SCO cobalt(II) compound provides new insight for the design of a new category of molecule-based magnetoelectric materials.

Multifunctional molecular materials exhibiting synergistic coexistence of two or more properties, have received considerable attention over recent years not only for their intrinsic interest but also because of their potential applications that include for information storage, sensors, spintronics and electro-optic devices.^[1–3] One of the more attractive multifunctional molecule-based materials for use in such applica-

tions are compounds that exhibit spin crossover (SCO) coupled with the occurrence of another phenomenon (or phenomena), for example, liquid crystalline behavior,^[4] electrical conductivity,^[5] luminescence^[6] and/or non-linear optical (NLO) properties.^[7] Molecular functional materials exhibiting both SCO behavior and ferroelectric property are of significant interest because of the potential that resulting magnetoelectric (ME) effects might be anticipated. However, to the best of our knowledge, there is a general lack of reports concerned with the synthesis and investigation of such ferroelectric SCO compounds.^[4,8] Recently in a solid-state SCO ferroelectric study it was shown that a hydrated iron(II) complex of type $[\text{Fe}(\text{bpp})_2](\text{isonic})_2 \cdot 2\text{H}_2\text{O}$ (bpp = 2,6-bis-(pyrazol-3-yl)pyridine; isonic = isonicotinate) was driven by structural transformation from a non-polar to polar space group through the removal of water.^[8] The above behavior reflects, first, that the switching of electronic configurations between low spin (LS) and high spin (HS) states is sensitive to subtle ligand field strength variation reflecting the occurrence of the structural perturbation. Secondly, the preparation of molecular ferroelectrics should meet the strict requirement that a compound must crystallize in a polar space group. As a consequence, the fabrication of molecular materials combining SCO and ferroelectricity has remained a formidable challenge.

In recent years, the use of molecular rotators as polarization rotation units has attracted increasing attention for the development of solid-state ferroelectric materials. For instance, Akutagawa et al. have reported that molecular ferroelectrics of type $(m\text{-FAni}^+)(\text{DB}[18]\text{crown-6})[\text{Ni}(\text{dmit})_2]^-$ ($m\text{-FAni}^+ = m\text{-fluoroanilinium}$; $\text{DB}[18]\text{crown-6} = \text{dibenzo}[18]\text{-crown-6}$; $\text{dmit}^{2-} = 2\text{-thioxo-1,3-dithiole-4,5-dithiolate}$) exhibits ferroelectricity by a 180° flip–flop motion of the $m\text{-FAni}^+$ cation.^[9] Subsequently, several types of ferroelectrics based on molecular motion have been synthesized.^[10] In these systems, appropriate molecular design leading to a large space for the molecular motion to occur has been of key importance. The introduction of such polarization rotation units into SCO compounds can not only produce ferroelectricity but can also affect SCO behavior at the metal centers, leading to the expression of ME effects.

Motivated by the above studies, we aimed to construct a new ferroelectric SCO compound whose ferroelectric properties originated from the presence of molecular motion. For this purpose, we synthesized a cobalt(II) complex, $[\text{Co}(\text{FPh-terpy})_2](\text{BPh}_4)_2$ (**1**; FPh-terpy = 4'-((3-fluorophenyl)ethynyl)-2,2':6,2''-terpyridine), in which each terpyridine ligand bears a fluorobenzene ring as a polarization rotation unit (Scheme 1). It was anticipated that the use of

[*] R. Akiyoshi, Y. Komatsumaru, Prof. Dr. S. Hayami
 Department of Chemistry, Graduate School of Science and Technology, Kumamoto University
 2-39-1 Kurokami, Chuo-ku, Kumamoto, 860-8555 (Japan)
 E-mail: hayami@kumamoto-u.ac.jp

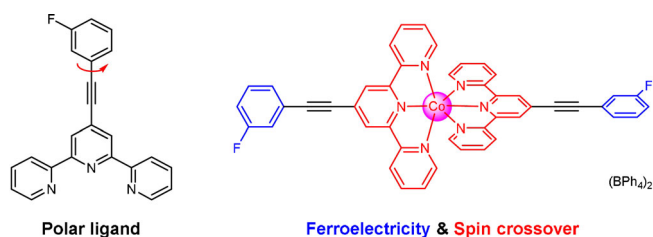
M. Donoshita, Dr. S. Dekura, Dr. Y. Yoshida, Prof. Dr. H. Kitagawa
 Division of Chemistry, Graduate School of Science, Kyoto University
 Kitashirakawa-Oiwakecho, Sakyo-ku, Kyoto 606-8502 (Japan)

Dr. Y. Kitagawa
 Division of Chemical Engineering, Department of Materials Engineering Science, Graduate School of Engineering Science, Osaka University
 1–3, Machikaneyama, Toyonaka, Osaka 560-8531 (Japan)

Prof. Dr. L. F. Lindoy
 School of Chemistry, The University of Sydney
 Sydney, NSW 2006 (Australia)

Prof. Dr. S. Hayami
 Institute of Industrial Nanomaterials (IINa), Kumamoto University
 2-39-1 Kurokami, Chuo-ku, Kumamoto, 860-8555 (Japan)

 Supporting information and the ORCID identification number(s) for the author(s) of this article can be found under:
<https://doi.org/10.1002/anie.202015322>



Scheme 1. Structures of polar ligand (left) and $[\text{Co}(\text{FPh-terpy})_2](\text{BPh}_4)_2$ (**1**) (right).

bulky BPh_4 anions might produce a large enough space in the lattice packing for molecular motion of fluorobenzene ring to occur, resulting in the generation of electrically invertible polarization. Related complexes of type $[\text{Co}(\text{Ph-terpy})_2](\text{BPh}_4)_2$ (**2**; Ph-terpy = 4'-(phenylethynyl)-2,2':6',2''-terpyridine), $[\text{Zn}(\text{FPh-terpy})_2](\text{BPh}_4)_2$ (**3**) and $[\text{Zn}(\text{Ph-terpy})_2](\text{BPh}_4)_2$ (**4**) were also prepared to compare their structures and properties with those of **1**.

The terpyridine ligand derivatives, FPh-terpy and Ph-terpy, were synthesized by minor modification of previously reported methods (Scheme S1).^[11] The complexes were synthesized by reaction of $\text{CoCl}_2 \cdot 6\text{H}_2\text{O}$ (or ZnCl_2), FPh-terpy (or Ph-terpy) and NaBPh_4 in MeOH; in each case the initial product was recrystallized from acetone to yield single crystals of **1-3ac**, **2-3ac**, **3-3ac** and **4-3ac** (where ac = acetone). Single crystal X-ray structures of each product were determined at 123 K. Crystallographic data are presented in Table S1. Compound **1-3ac** crystallized in the low crystal symmetry of $P2_1/c$ (centrosymmetric space group). As shown in Figure 1, two FPh-terpy ligands coordinate to the cobalt(II)

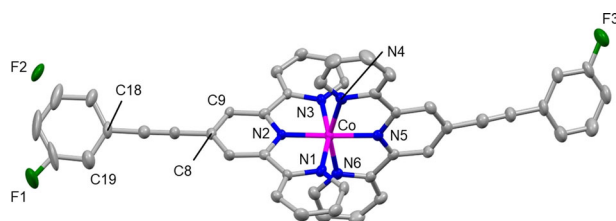


Figure 1. Crystal structure of **1-3ac** showing the F1/F2 disorder. Counter anions, H atoms and solvent molecules are omitted for clarity. Color code: Co; magenta, C; grey, N; blue, F; green.^[15]

center meridionally to yield a N_6 donor set. The Co–N bond lengths are 1.999(3) Å, 1.858(3) Å, 2.013(3) Å, 2.128(3) Å, 1.905(3) Å and 2.122(3), in accord with **1-3ac** being in its LS state (Table S2). One fluorobenzene moiety is distorted with respect to the terpyridine plane due to a CH– π interaction with a neighboring ligand, with a $\text{H25} \cdots \text{C43}$ distance of 2.825 Å, while the second (bound) FPh-terpy ligand has a planar structure due to the absence of such an intermolecular interaction (Figure S1). The bulky tetraphenylborate anions surround the fluorobenzene ring to produce an open space that is sufficient to allow molecular motion of the fluorobenzene ring (Figure S2). The fluorine substituent is disordered over two sites, F1 and F2. The occupation (occ) ratio between F1 and F2 is 1.2:1 at 123 K, where the

intermolecular interaction between F1 site and neighboring ac molecule causes the biased-population (Figure S3). Variable-temperature SXR (VT-SXR) measurements were performed to examine the effect on the degree of occ at the F1 and F2 sites. On increasing the temperature above 123 K, the occ increased at the F1 site but decreased for the F2 site accompanied by the disorder of neighboring ac molecule, consequently reaching 1.6:1 (F1:F2) at 293 K (Table 1). These

Table 1: Changes in the occupation (occ) factor at the F1 and F2 sites of fluorobenzene ring obtained from the VT-SXR analyses.

T [K]	occ F1 site	occ F2 site	F1:F2
123	0.55	0.45	1.2:1
170	0.55	0.45	1.2:1
220	0.56	0.44	1.3:1
293	0.61	0.39	1.6:1

results clearly demonstrate that raising the temperature increases the 180° flip–flop motion of the fluorobenzene ring. The average Co–N bond lengths (2.034 Å) at 293 K also indicates the presence of thermally-induced SCO behavior (Table S2). Above temperature-dependent structural variation that includes F1:F2 occ ratio and Co–N bond length is fully reversible in the temperature range 123 to 293 K. The crystal structures of **2-3ac**, **3-3ac** and **4-3ac**, determined at 123 K, are isostructural with that of **1-3ac** (Figure S4, S5 and S6). For **3-3ac**, the fluorine group disorder was observed with an F1:F2 occ ratio of 1.2:1, similar to that observed for **1-3ac**. The lattice ac molecules were gradually removed at 298 K, and the structures were maintained up to ca. 350 K as confirmed by thermogravimetric analysis (TGA) and variable-temperature powder X-ray diffraction (VT-PXRD) patterns (Figure S7 and S8). Hence, all temperature-dependent measurements were carried out below 350 K.

In order to further investigate the molecular motion of fluorobenzene ring, we measured the temperature-dependent, solid-state ^{19}F nuclear magnetic resonance (SS- ^{19}F NMR) spectra for **3-3ac** (Figure 2a). As presented in Figure 2b, two signals were present at ca. –83.1 and –50.0 ppm. These signals are assigned to the F1, F2 and F3 atoms as observed by SXR analyses, with the ratio of F1 and F2 being 1.2:1 at 150 K. On heating from 150 K, the signal intensity increases for F1 while decreasing for F2 and reaches the ratio of 1.6:1 at 298 K (Figure 2c). Such behavior is in full accord with the presence of thermally-induced molecular motion of the fluorobenzene ring in each complex, and is also consistent with the change in degree of occ occurring at the F1 and F2 sites obtained from the VT-SXR analyses of **1-3ac** (Figure S9).

The molecular motion of phenyl ring was revealed by means of SS- ^1H NMR spectroscopy for **4-3ac** and SS- ^2H NMR spectroscopy for deuterated **4-3ac** on phenyl moiety. Temperature-dependent SS- ^1H NMR spectra for **4-3ac** is shown in Figure S10. At 180 K, two signals centered at ca. 6.0 ppm and ca. 1.0 ppm were evident. When the temperature varied from 180 to 250 K, new sharp signal centered at ca. 5.0 ppm starts to be appearance at 200 K and

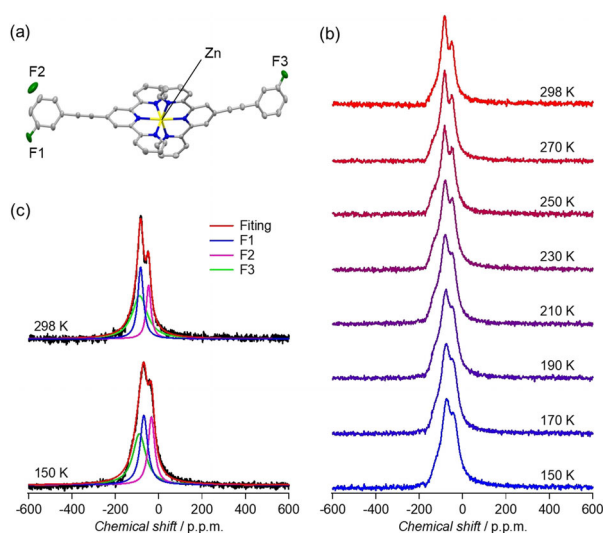


Figure 2. a) F1, F2 and F3 sites in **3-3ac**. b) Temperature-dependent SS-¹⁹F NMR spectra of **3-3ac**. c) Fitting results for spectra at 150 K and 298 K, respectively (blue: F1, magenta: F2, green: F3, red: fitting line).

the original signal at ca. 1.0 ppm gradually become broader over 230 K. Although we cannot assign each signal, it is thought that the observed spectral change between 200 and 250 K relates to the thermally-induced molecular motion of phenyl ring in **4-3ac**. The SS-²H NMR spectra for deuterated **4-3ac** on phenyl moiety, [Zn(Ph-*d*₅-terpy)₂](BPh₄)₂, also supported the presence of molecular motion of phenyl ring. The spectra vary progressively with increasing temperature and are successfully simulated by taking into account of two-site 180° flip-flop motion of phenyl ring with the aid of software NMR WEBLAB (Figure 3a).^[12] At 190 K, the spectrum was reproduced well with the flipping rate (*k*) being 1.0 × 10³ Hz, indicating slow flip-flop motion of the phenyl ring. On heating from 190 K, the spectral shape starts to change at ca. 230 K (*k* = 2.0 × 10⁴ Hz) as indicated by arrows and reaches *k* value of 7.9 × 10⁶ Hz at 306 K. The temperature at which the spectral change starts to emerge in SS-²H NMR spectra is consistent with the temperature of the fluorine-group occ change resulted from SXRD and SS-¹⁹F NMR spectra, thus suggesting that **4-3ac** (which has no fluorine group) exhibits the similar thermally-activated molecular motion to **3-3ac** (which has fluorine group). The *k* vs. 1000 *T*⁻¹ plot is shown in Figure 3b. From this linear plot, the activation energy (*E*_a) was estimated to be 36.2 kJ mol⁻¹ by using the Arrhenius equation, $\tau^{-1} = \tau_0^{-1} \exp(-E_a/k_B T)$. This value is quite similar to that of 180° flip-flop motion of phenyl ring in molecular rotor based on [18]crown-6.^[13]

The rotational potential energy in **1-3ac** was calculated by using the B3LYP-D3BJ/(F:6-31 + G* others:6-31G*) level of theory and atomic coordinates at 123 K. Computational details for the calculation are shown in Table S3. The single point energy for the forward-backward rotation of fluorobenzene ring was plotted against the dihedral angle C9-C8-C18-C19 (ϕ) with taking into account of intermolecular contacts with surrounding molecules (Figure S11). The ϕ value of the initial structure obtained from SXRD analysis is 142.3°, where the ΔE value is defined as 0 kJ mol⁻¹. As a result

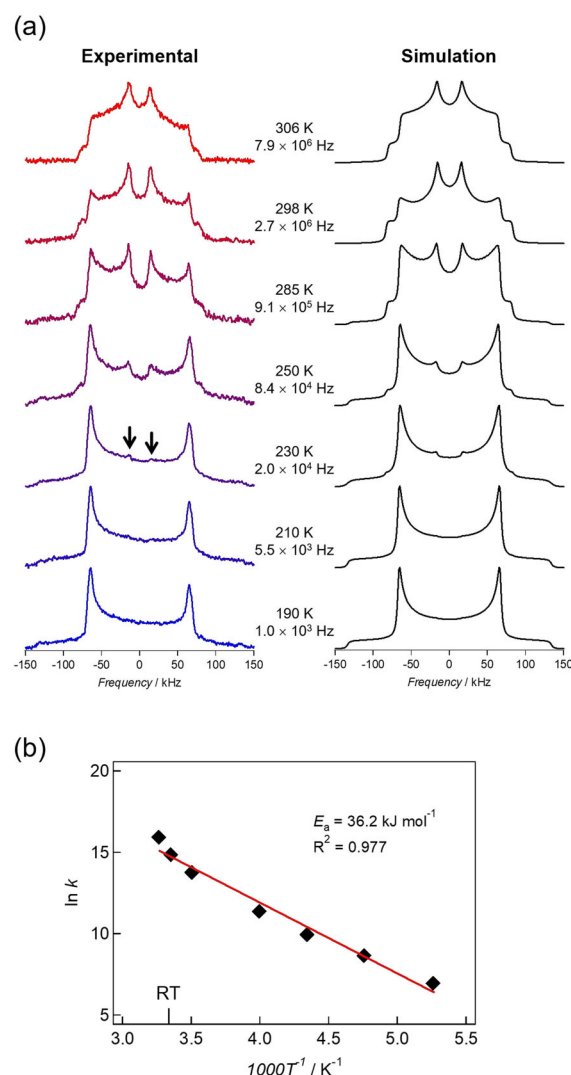


Figure 3. a) Temperature-dependent SS-²H NMR spectra for deuterated **4-3ac** on phenyl ring moiety (left: experimental, right: simulation). b) Arrhenius plot of ln(*k*) vs. 1000 *T*⁻¹.

of calculation, two potential energy barriers were observed centered at $\phi = -134$ and 33°, with the ΔE being 254.3 and 457.9 kJ mol⁻¹, respectively (red plot in Figure 4). The respective ΔE maxima are attributed to the intermolecular contacts with neighboring acetone molecule and [Co(Ph-terpy)₂] cation (Figure S12). The value of $k_B T$ (k_B = Boltzmann constant) is 2.8 kJ mol⁻¹ at 298 K, which is significantly smaller than the ΔE maxima observed (for **1-3ac**). Undoubtedly, this indicates that the rotation of the fluorobenzene will be almost suppressed at 298 K. Hence, **1-3ac** is expected to display a remnant polarization after removing the electric field. Compound **2-3ac** also gave a double potential curve (blue plot in Figure 4). Since the two symmetric potential energy barriers (157.0 and 155.2 kJ mol⁻¹) observed in **2-3ac** are lower than occur for **1-3ac**, the intermolecular contacts involving the fluorine group clearly lead to increased potential energy barriers. The calculated potential energy barrier for **2-3ac** is 4.3 times as large as the *E*_a value obtained from SS-²H NMR spectroscopy. It should be emphasized that

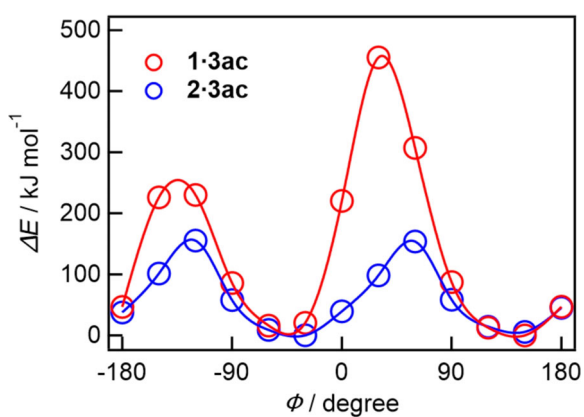


Figure 4. Calculated potential energy curves and dihedral angle C9-C8-C18-C19 (ϕ) for the fluorobenzene (phenyl) ring in a) **1-3ac** and b) **2-3ac**. The single point energies for the model structures (Figure S11) were calculated for every 30° rotation.

the calculated potential energy barriers are overestimated to the experimental data because atomic coordinates are fixed to the SXR structure measured at 123 K except for the dihedral angle, and no structural relaxation due to the rotation is considered.

The 180° flip-flop motion of the fluorobenzene ring has the potential to induce ferroelectric properties. The temperature dependences of the dielectric constants (ϵ_r) for **1-3ac** and **2-3ac** were measured on a pellet sample in the frequency range 0.1 kHz to 1 MHz in order to investigate any phase transition/electric field effects. With increasing temperature, the dielectric constant for **1-3ac** is nearly constant between 200 and 240 K, but then gradually increases in accord with the fluorine-group occ change taking place (above plot in Figure 5a). The dielectric constant for **1** at higher frequency is significantly smaller than that observed at 0.1 kHz, undoubtedly indicating that the rotation of the fluorobenzene ring is unable to fully respond to the electric field owing to the latter's higher frequency. For **2-3ac** (which has no fluorine group), no elevation of the dielectric constant was evident between 200 and 350 K due to the absence of dipole moment (plot below in Figure 5a). The ferroelectric behaviors origi-

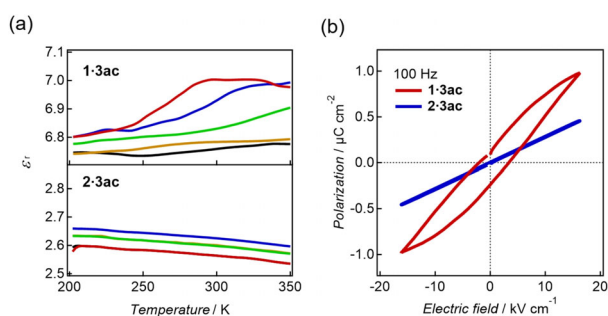


Figure 5. a) Temperature- and frequency-dependent dielectric constants (ϵ_r) of **1-3ac** and **2-3ac** using pellet samples (red: 0.1 kHz, blue: 1 kHz, green: 10 kHz, yellow: 100 kHz, black: 1000 kHz). b) P - E hysteresis curves for **1-3ac** (red) and **2-3ac** (blue) at 298 K. The frequency employed for generating the data for the P - E curves was fixed at 100 Hz and was obtained using pellet sample.

inating from the molecular rotation were analyzed for the pellet sample using polarization vs. electric field (P - E) curves with the aid of a TF analyzer1000 ($T=298$ K, $f=100$ Hz). Compound **1-3ac** displayed a distinct ferroelectric hysteresis loop, with the remnant polarization being 0.24 μC —a typical value for ferroelectric compounds (red line in Figure 5b). The distinct frequency dependence was found in ferroelectric hysteresis loop, which is typical nature of ferroelectric compound (Figure S13). In the temperature-dependent P - E curves, no ferroelectric hysteresis loop was evident below 200 K because of the small-degree of biased-population ($1.2:1 \leq F1:F2$) or frozen molecular motion at low temperature (Figure S14). This result is undoubtedly consistent with temperature dependence of dielectric constants. In general, ferroelectric behavior stems from non-centrosymmetric group. In the present case, such behavior, however, occurred in the centrosymmetric compound ($P2_1/c$). This situation is quite similar to ferroelectric molecular rotor reported by Akutagawa et al.^[9] Thus, it is likely that the biased occ factor (1.6:1) of fluorine group in the initial structure transforms to the more biased population after applying an electric field (Figure S15). As expected, no ferroelectric hysteresis loop resulting in ferroelectricity was observed for **2-3ac** (blue line in Figure 5b). Collectively, these results clearly indicate that the invertible polarization necessary for ferroelectricity is generated via the rotational motion of the fluorobenzene ring in **1-3ac**.

SCO behaviors of **1-3ac** and **2-3ac** were investigated employing a Superconducting Quantum Interference Device (SQUID) in the temperature range 5 to 350 K at 5 K min^{-1} (Figure 6). In general, an octahedral cobalt(II) complex shows spin conversion between $S=1/2$ ($t_{2g}^6 e_g^1$) and $S=3/2$ ($t_{2g}^5 e_g^2$) with the $\chi_m T$ for the LS state being around 0.5 $\text{cm}^3 \text{K mol}^{-1}$ and for the HS state being in the range 1.7–3.0 $\text{cm}^3 \text{K mol}^{-1}$ (reflecting the contribution of orbit angular momentum). Compounds **1-3ac** and **2-3ac** each undergo

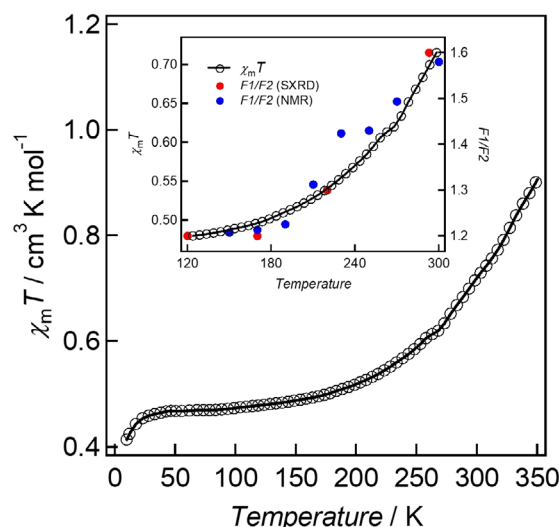


Figure 6. Temperature-dependent magnetic susceptibility data for **1-3ac** collected in the range 5–350 K under an applied field of 0.5 T. Inset graph displays $\chi_m T$ and $F1/F2$ vs. T plots (red: SXR for **1-3ac**, blue: SS- ^{19}F NMR for **3-3ac**).

incomplete SCO behavior between 5 and 350 K. For **1-3ac**, the $\chi_m T$ value of $0.41 \text{ cm}^3 \text{ K mol}^{-1}$ at 5 K, clearly indicates the LS state for cobalt(II). Upon heating from 5 K, the $\chi_m T$ value remains essentially constant between 5 and ≈ 200 K. Subsequently, the $\chi_m T$ value gradually rises to $0.71 \text{ cm}^3 \text{ K mol}^{-1}$ at 300 K, followed by an increase to $0.90 \text{ cm}^3 \text{ K mol}^{-1}$ at 350 K. Similar SCO behavior was observed for **2-3ac** (Figure S16). The $\chi_m T$ value at 5 K is $0.44 \text{ cm}^3 \text{ K mol}^{-1}$ and starts to increase at ≈ 200 K to reach $0.89 \text{ cm}^3 \text{ K mol}^{-1}$ at 350 K. The temperatures at which the $\chi_m T$ values start to increase in **1-3ac** and **2-3ac** are in accordance with the thermally-induced 180° flip-flop motion obtained from SS-NMR spectra for **3-3ac**, **4-3ac** and deuterated **4-3ac** (Figure 6 inset). Thus, in each case the behavior is in keeping with structural changes associated with the molecular motion of the respective aromatic rings. In general, SCO is an entropy-driven phenomenon, in which the LS state is the ground state at low temperature whereas the HS state becomes the ground state at high temperature. The difference in energy is thermally compensated by the higher entropy of the HS state, which mainly stems from electronic and vibrational contributions. In the present case, the change in rotation velocity of the fluorobenzene ring may contribute considerably to this entropy variation, consequently influencing the SCO process. Thus, LS state is favorable at low temperature due to the restricted mobility of fluorobenzene (phenyl) ring while showing HS state at high temperature owing to the acquirement of entropy occurring from the mobility of the fluorobenzene (phenyl) ring. A similar example of SCO behavior being triggered by the degree of rotation velocity has also been reported by Rodríguez-Velamazán et al.^[14]

In conclusion, herein we report the synthesis and investigation of a cobalt(II) complex (**1**) exhibiting SCO behavior that is dependent on the degree of molecular motion of the FPh-terpy ligand's fluorophenyl ring. Variable-temperature SXRD analyses and SS-¹⁹F NMR spectra confirmed the presence (as well as the effect) of the 180° flip-flop motion of the fluorobenzene ring. The flip-flop motion also results in an electrically reversible dipole moment that in turn leads to the generation of a ferroelectric hysteresis loop and spontaneous polarization. This first example of the SCO behavior associated with the polar aromatic ring motion clearly provides new insight for the design and synthesis of further ME materials in the future.

Acknowledgements

This work was supported by KAKENHI Grant-in-Aid for Scientific Research (A) JP17H01200. R.A. is grateful to JSPS Research Fellowships for Young Scientists (JP20J11519).

Conflict of interest

The authors declare no conflict of interest.

Keywords: cobalt(II) complexes · ferroelectrics · molecular rotors · spin crossover

- [1] a) P. Silva, S. M. Vilela, J. P. Tome, F. A. Almeida Paz, *Chem. Soc. Rev.* **2015**, *44*, 6774–6803; b) C. L. Ho, Z. Q. Yu, W. Y. Wong, *Chem. Soc. Rev.* **2016**, *45*, 5264–5295.
- [2] a) M. Castellano, R. Ruiz-García, J. Cano, J. Ferrando-Soria, E. Pardo, F. R. Fortea-Pérez, S.-E. Stiriba, W. P. Barros, H. O. Stumpf, L. Cañadillas-Delgado, J. Pasán, C. Ruiz-Pérez, G. de Munno, D. Armentano, Y. Journaux, F. Lloret, M. Julve, *Coord. Chem. Rev.* **2015**, *303*, 110–138; b) Y. He, B. Li, M. O'Keefe, B. Chen, *Chem. Soc. Rev.* **2014**, *43*, 5618–5656; c) M. K. Singh, Y. Yang, C. G. Takoudis, *Coord. Chem. Rev.* **2009**, *253*, 2920–2934.
- [3] a) E. Chelebaeva, J. Larionova, Y. Guari, R. A. Ferreira, L. D. Carlos, F. A. Paz, A. Trifonov, C. Guérin, *Inorg. Chem.* **2009**, *48*, 5983–5995; b) R. Hao, R. Xing, Z. Xu, Y. Hou, S. Gao, S. Sun, *Adv. Mater.* **2010**, *22*, 2729–2742; c) J. Long, J. Rouquette, J. M. Thibaud, R. A. Ferreira, L. D. Carlos, B. Donnadiou, V. Vieru, L. F. Chibotaru, L. Konczewicz, J. Haines, Y. Guari, J. Larionova, *Angew. Chem. Int. Ed.* **2015**, *54*, 2236–2240; *Angew. Chem.* **2015**, *127*, 2264–2268.
- [4] a) S. Hayami, R. Moriyama, A. Shuto, Y. Maeda, K. Ohta, K. Inoue, *Inorg. Chem.* **2007**, *46*, 7692–7694; b) M. Seredyuk, A. B. Gaspar, V. Ksenofontov, Y. Galyametdinov, J. Kusz, P. Gütllich, *Adv. Funct. Mater.* **2008**, *18*, 2089–2101; c) M. Seredyuk, A. B. Gaspar, V. Ksenofontov, Y. Galyametdinov, J. Kusz, P. Gütllich, *J. Am. Chem. Soc.* **2008**, *130*, 1431–1439; d) A. B. Gaspar, M. Seredyuk, P. Gütllich, *Coord. Chem. Rev.* **2009**, *253*, 2399–2413; e) M. Seredyuk, M. C. Muñoz, V. Ksenofontov, P. Gütllich, Y. Galyametdinov, J. A. Real, *Inorg. Chem.* **2014**, *53*, 8442–8454; f) R. Akiyoshi, Y. Hirota, D. Kosumi, M. Tsutsumi, M. Nakamura, L. F. Lindoy, S. Hayami, *Chem. Sci.* **2019**, *10*, 5843–5848.
- [5] a) C. Faulmann, K. Jacob, S. Dorbes, S. Lampert, I. Malfant, M.-L. Doublet, L. Valade, J. A. Real, *Inorg. Chem.* **2007**, *46*, 8548–8559; b) K. Takahashi, H.-B. Cui, Y. Okano, H. Kobayashi, H. Mori, H. Tajima, Y. Einaga, O. Sato, *J. Am. Chem. Soc.* **2008**, *130*, 6688–6689; c) M. Nihei, N. Takahashi, H. Nishikawa, H. Oshio, *Dalton Trans.* **2011**, *40*, 2154–2156; d) T. Mahfoud, G. Molnár, S. Cobo, L. Salmon, C. Thibault, C. Vieu, P. Demont, A. Bousseksou, *Appl. Phys. Lett.* **2011**, *99*, 053307; e) A. Rotaru, I. A. Gural'skiy, G. Molnár, L. Salmon, P. Demont, A. Bousseksou, *Chem. Commun.* **2012**, *48*, 4163–4165; f) H. Phan, S. M. Benjamin, E. Steven, J. S. Brooks, M. Shatruk, *Angew. Chem. Int. Ed.* **2015**, *54*, 823–827; *Angew. Chem.* **2015**, *127*, 837–841.
- [6] a) I. Suleimanov, O. Kraieva, J. Sánchez Costa, I. O. Fritsky, G. Molnár, L. Salmon, A. Bousseksou, *J. Mater. Chem. C* **2015**, *3*, 5026–5032; b) A. Santoro, L. J. Kershaw Cook, R. Kulmaczewski, S. A. Barrett, O. Cespedes, M. A. Halcrow, *Inorg. Chem.* **2015**, *54*, 682–693; c) C. F. Wang, R. F. Li, X. Y. Chen, R. J. Wei, L. S. Zheng, J. Tao, *Angew. Chem. Int. Ed.* **2015**, *54*, 1574–1577; *Angew. Chem.* **2015**, *127*, 1594–1597; d) J. L. Wang, Q. Liu, X. J. Lv, R. L. Wang, C. Y. Duan, T. Liu, *Dalton Trans.* **2016**, *45*, 18552–18558; e) M. Estrader, J. Salinas Uber, L. A. Barrios, J. Garcia, P. Lloyd-Williams, O. Roubeau, S. J. Teat, G. Aromi, *Angew. Chem. Int. Ed.* **2017**, *56*, 15622–15627; *Angew. Chem.* **2017**, *129*, 15828–15833; f) J.-Y. Ge, Z. Chen, L. Zhang, X. Liang, J. Su, M. Kurmoo, J.-L. Zuo, *Angew. Chem. Int. Ed.* **2019**, *58*, 8789–8793; *Angew. Chem.* **2019**, *131*, 8881–8885; g) B. Benaicha, K. V. Do, A. Yangui, N. Pittala, A. Lussan, M. Sy, G. Bouchez, H. Fourati, C. J. Gomez-Garcia, S. Triki, K. Boukheddaden, *Chem. Sci.* **2019**, *10*, 6791–6798.
- [7] a) A. B. Gaspar, V. Ksenofontov, M. Seredyuk, P. Gütllich, *Coord. Chem. Rev.* **2005**, *249*, 2661–2676; b) S. Bonhommeau, P. G. Lacroix, D. Talaga, A. Bousseksou, M. Seredyuk, I. O. Fritsky, V. Rodriguez, *J. Phys. Chem. C* **2012**, *116*, 11251–11255;

- c) P. G. Lacroix, I. Malfant, J.-A. Real, V. Rodriguez, *Eur. J. Inorg. Chem.* **2013**, 615–627; d) S.-i. Ohkoshi, S. Takano, K. Imoto, M. Yoshikiyo, A. Namai, H. Tokoro, *Nat. Photonics* **2014**, *8*, 65–71; e) W. Liu, X. Bao, L. L. Mao, J. Tucek, R. Zboril, J. L. Liu, F. S. Guo, Z. P. Ni, M. L. Tong, *Chem. Commun.* **2014**, *50*, 4059–4061.
- [8] V. Jornet-Mollá, Y. Duan, C. Giménez-Saiz, Y.-Y. Tang, P.-F. Li, F. M. Romero, R.-G. Xiong, *Angew. Chem. Int. Ed.* **2017**, *56*, 14052–14056; *Angew. Chem.* **2017**, *129*, 14240–14244.
- [9] T. Akutagawa, H. Koshinaka, D. Sato, S. Takeda, S. Noro, H. Takahashi, R. Kumai, Y. Tokura, T. Nakamura, *Nat. Mater.* **2009**, *8*, 342–347.
- [10] a) D.-W. Fu, W. Zhang, H.-L. Cai, Y. Zhang, J.-Z. Ge, R.-G. Xiong, S. D. Huang, *J. Am. Chem. Soc.* **2011**, *133*, 12780–12786; b) S. Kushida, E. Smarsly, N. M. Bojanowski, I. Wacker, R. R. Schroder, O. Oki, Y. Yamamoto, C. Melzer, U. H. F. Bunz, *Angew. Chem. Int. Ed.* **2018**, *57*, 17019–17022; *Angew. Chem.* **2018**, *130*, 17265–17268.
- [11] a) K. T. Potts, D. Konwar, *J. Org. Chem.* **1991**, *56*, 4815–4816; b) S. Ott, M. Borgström, M. Kritikos, R. Lomoth, J. Bergquist, B. Akermark, L. Hammarström, L. Sun, *Inorg. Chem.* **2004**, *43*, 4683–4692; c) G. Du, E. Moulin, N. Jouault, E. Buhler, N. Giuseppone, *Angew. Chem. Int. Ed.* **2012**, *51*, 12504–12508; *Angew. Chem.* **2012**, *124*, 12672–12676.
- [12] V. Macho, L. Brombacher, H. W. Spiess, *Appl. Magn. Reson.* **2001**, *20*, 405–432.
- [13] S. Nishihara, T. Akutagawa, D. Sato, S. Takeda, S. Noro, T. Nakamura, *Chem. Asian J.* **2007**, *2*, 1083–1090.
- [14] J. A. Rodríguez-Velamazán, M. A. González, J. A. Real, M. Castro, M. C. Muñoz, A. B. Gaspar, R. Ohtani, M. Ohba, K. Yoneda, Y. Hijikata, N. Yanai, M. Mizuno, H. Ando, S. Kitagawa, *J. Am. Chem. Soc.* **2012**, *134*, 5083–5089.
- [15] Deposition Number(s) 1889884, 1889885, 1889886 and 2022098 contain(s) the supplementary crystallographic data for this paper. These data are provided free of charge by the joint Cambridge Crystallographic Data Centre and Fachinformationszentrum Karlsruhe Access Structures service www.ccdc.cam.ac.uk/structures.

Manuscript received: November 18, 2020

Revised manuscript received: March 12, 2021

Accepted manuscript online: March 12, 2021

Version of record online: ■■■■■■, ■■■■■■

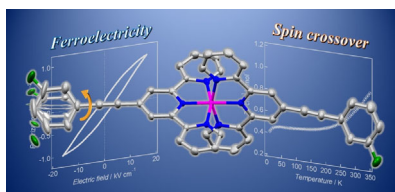
Communications



Ferroelectrics

R. Akiyoshi, Y. Komatsumaru,
M. Donoshita, S. Dekura, Y. Yoshida,
H. Kitagawa, Y. Kitagawa, L. F. Lindoy,
S. Hayami* ————— ■■■■—■■■■

Ferroelectric and Spin Crossover Behavior
in a Cobalt(II) Compound Induced by
Polar-Ligand-Substituent Motion



Inspired by molecular ferroelectrics induced by molecular rotors, multifunctional compound exhibiting both ferroelectricity and spin crossover behavior was constructed. The flip-flop motion of polarization unit results in the expression of ferroelectricity and spin crossover behavior.